Mono(pentamethylcyclopentadienyl)tantalum Complexes Containing a Structurally Versatile Enediamido(2−) Ligand

Hiroyuki Kawaguchi, Yoshiaki Yamamoto, Keiko Asaoka, and Kazuyuki Tatsumi*

Research Center for Materials Science and Department of Chemistry, Graduate School of Science, Nagoya University, Furo-cho, Chikusa-ku, Nagoya 464-8602, Japan

Received April 27, 1998

Treatment of Cp*$TaCl_4$ with 1 equiv of $Li_2(R_2$-dad) in THF afforded Cp*Ta(R_2-dad)Cl_2 (R = ^{i}Pr (**1**), ^{t}Bu (**2**)). The chlorido ligands of **1** and **2** reacted smoothly with 2 equiv of LiC≡C^{t}Bu, MeMgI and LiS^{t}Bu, resulting in Cp*Ta(R_2-dad)(C≡C^{t}Bu)$_2$ (R = ^{i}Pr (**3**), ^{t}Bu (**4**)), Cp*Ta(R_2-dad)Me_2 (R = ^{i}Pr (**5**), ^{t}Bu (**6**)), and Cp*Ta(^{t}Bu$_2$-dad)(S^{t}Bu)$_2$ (**7**), respectively. The X-ray analyses of **1**, **3**, **4**, **5**, and **7** have been carried out. In the structures of **1**, **3**, **4**, and **5**, the R_2-dad ligand is bound to the metal center with a $\sigma^2(N,N')$, $\pi(C,C')$-coordination mode, which opts for a supine conformation with respect to the Cp* group for **1** and **3**, while an alternative prone conformation is adopted for **4** and **5**. In contrast, the ^{t}Bu$_2$-dad ligand of **7** assumes an intriguing $\eta^2(N,C)$ coordination geometry. Treatment of **7** in toluene at 80 °C was found to induce C−S bond cleavage of the thiolates generating Cp*Ta(^{t}Bu$_2$-dad)(S) (**8**), in which the dad ligand resumes a σ^2, π-coordination geometry with a prone conformation.

Introduction

The recent development of organometallic chemistry of early transition metals owes much to evolution of metallocene systems. The wedge-shaped bis-cyclopentadienylmetal fragments provide geometrically well-defined pockets, the size and the shape of which are suited for the promotion of various important organic/inorganic reactions.[1] To expand the scope of metallocene chemistry, it is desirable to finely tune the geometry of reaction sites. Introduction of sophisticated substituents and/or use of ring-bridged bis-cyclopentadienyl ligands are strategies employed for modification of the parent cyclopentadienyl ring.[2] If one cyclopentadienyl group of metallocene is replaced by a geometrically flexible ancillary ligand, yet another range of new reactive sites may be created.

In this context, we have been interested in N,N′-disubstituted diazabutadiene (R_2-dad). The use of R_2-dad has 3-fold advantages: (1) they exhibit versatile coordination modes ranging from η^1-N, to η^2-N,N′, to η^2-N,C, and to η^4-N_2C_2 (σ^2,π); (2) they are also electronically flexible, acting as either neutral ligands or dianion (enediamido) ligands;[3] (3) their steric size can be regulated by N-substituents. A large number of R_2-dad complexes of late transition metals are known, and the R_2-dad moieties coordinate at metals mostly as neutral ligands. Although the number of early transition metal analogues is increasing, where R_2-dad ligands usually favor dianionic forms, their chemistry has yet to be explored.[4−7] One of the most intriguing examples of this class may be Nb(^{t}Bu$_2$-dad)$_3$Li and Nb$_2$(^{t}Bu$_2$-dad)$_5$ prepared by Thiele and co-workers, in which the dad ligands are bound to the metal centers in a variety of forms.[8]

In this paper, we report the synthesis and structures of a series of tantalum complexes consisting of a common Cp*Ta(R_2-dad) fragment (Cp* = η^5-C_5Me_5;

(1) *Comprehensive Organometallic Chemistry II*; Abel, E. W., Stone, F. A., Wilkinson, G., Eds.; Pergamon Press: Oxford, U.K., 1995; Vol. 4.

(2) (a) Kravchenko, R.; Masood, A.; Waymouth, R. M.; Myers, C. L. *J. Am. Chem. Soc.* **1998**, *120*, 2039−2046. (b) Kiely, A. F.; Nelson, C. M.; Pastor, A.; Henling, L. M.; Day, M. W.; Bercaw, J. E. *Organometallics* **1998**, *17*, 1324−1332. (c) Jaquith, J. B.; Levy, C. J.; Bondar G. V.; Wang, S.; Collins, S. *Organometallics* **1998**, *17*, 914−925. (d) Sinnema, P.-J.; van der Veen, L.; Spek, A. L.; Veldman, N.; Teuben, J. H. *Organometallics* **1997**, *16*, 4245−4247, and references therein.

(3) (a) *Comprehensive Coordination Chemistry*; Wilkinson, G., Gillard, R. D., McCleverty, J. A., Eds.; Pergamon Press: Oxford, U.K., 1987; Vol. 2. (b) Vrieze, K. *J. Organomet. Chem.* **1986**, *300*, 307−326. (c) Vrieze, K.; van Koten, G. *Adv. Organomet. Chem.* **1982**, *21*, 151−239.

(4) (a) Görls, H.; Neumüller, B.; Scholz, A.; Scholz, J. *Angew. Chem., Int. Ed. Engl.* **1995**, *34*, 673−676. (b) Scholz, A.; Thiele, K.-H.; Scholz, J.; Weimann, R. *J. Organomet. Chem.* **1995**, *501*, 195−200. (c) Bochkarev, M. N.; Trifonov, A. A.; Cloke, F. G. N.; Dalby, C. I.; Matsunaga, P. T.; Anderson, R. A.; Schumann, H.; Loebel, J.; Hemling, H. *J. Organomet. Chem.* **1995**, *486*, 177−182.

(5) (a) Scholz, J.; Dietrich, A.; Schumann, H.; Thiele, K.-H. *Chem. Ber.* **1991**, *124*, 1035−1039. (b) Thiele, K.-H.; Richter, B.; Neumüller, B. *Z. Anorg. Allg. Chem.* **1994**, *620*, 1627−1630. (c) Scholz, J.; Dlikan, M.; Ströhl, D.; Dietrich, A.; Schumann, H.; Thiele, K. H. *Chem. Ber.* **1990**, *123*, 2279−2285. (d) Herrmann, W. A.; Denk, M.; Scherer, W.; Klingan, F.-R. *J. Organomet. Chem.* **1993**, *444*, C21−C24. (e) tom Dieck, H.; Rieger, H. J.; Fendesak, G. *Inorg. Chem. Acta* **1990**, *177*, 191−197. (f) Woitha, C.; Behrens, U.; Vergopoulos, V.; Rehder, D. *J. Organomet. Chem.* **1990**, *393*, 97−109. (g) Chamberlain, L. R.; Durfee, L. D.; Fanwick, P. E.; Kobriger, L, M.; Latesky, S. L.; McMullen, A. K.; Steffey, B. D.; Rothwell, I. P.; Folting, K.; Huffman, J. C. *J. Am. Chem. Soc.* **1987**, *109*, 6068−6076. (h) Latesky, S. L.; McMullen, A. K.; Niccolai, G. P.; Rothwell, I. P.; Huffman, J. C. *Organometallics* **1985**, *4*, 1896−1898.

(6) Hessen, B.; Bol, J. E.; de Boer, J. L.; Meetsma, A.; Teuben, J. H. *J. Chem. Soc., Chem. Commun.* **1989**, 1276−1277.

(7) Hubert-Pfalzgraf, L. G.; Zaki, A. *Acta Crystallogr.* **1993**, *C49*, 1609−1611.

(8) Richter, B.; Scholz, J.; Sieler, J.; Thiele, K.-H. *Angew. Chem., Int. Ed. Engl.* **1995**, *34*, 2649−2651.

S0276-7333(98)00319-7 CCC: $15.00
Publication on Web 09/01/1998

R = ^{t}Bu, ^{i}Pr). Our study demonstrates that the coordination geometries of R_2-dad are determined by a delicate balance of steric (and/or electronic) factors of the R groups and incoming ligands. Recently the synthesis of Cp*Ta{$(C_6H_4-OCH_3\text{-p})_2$-dad}$Cl_2$ and Cp*Ta{$(C_6H_4-OCH_3\text{-p})_2$-dad}($\eta^4$-1,3-butadiene) has appeared.[9]

Results and Discussion

Synthesis of Cp*Ta(R_2-dad)Cl_2 (R = ^{i}Pr (1), ^{t}Bu (2)). The R_2-dad ligands (R = ^{i}Pr, ^{t}Bu) were introduced successfully into the half-sandwich tantalum fragment by treating Cp^*TaCl_4 with $Li_2(R_2\text{-dad})$, which was prepared by the reaction of excess Li with R_2-dad in THF.[10] The red THF solution of $Li_2(R_2\text{-dad})$ was used in the synthesis of the Ta complexes reported here, although we found that the dilithium salts of R_2-dad could be isolated as THF adducts.[5a] Treatment of Cp^*TaCl_4 with 1 equiv of $Li_2(R_2\text{-dad})$ in THF afforded Cp*Ta(R_2-dad)Cl_2 (R = ^{i}Pr (**1**), ^{t}Bu (**2**)). The compound **1** is poorly soluble in common organic solvents, and it can easily be separated out from the reaction system as yellow microcrystalline precipitates. On the other hand, **2** is very soluble in THF and is best recrystallized from DME. Both **1** and **2** are relatively stable in solid and decompose slowly by prolonged exposure to air, while their CH_2Cl_2 (or $CHCl_3$) solutions are highly unstable.

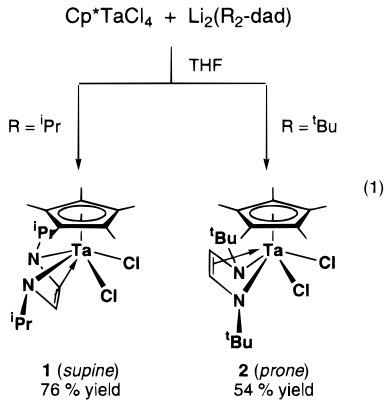

Spectroscopic data and combustion analyses of **1** and **2** are in agreement with the formulations. Their ^{1}H NMR spectra in toluene-d_8 are essentially invariant in the temperature range from −50 to 90 °C. In each spectrum, the Cp* proton signal appears as a singlet (**1**, δ 2.07; **2**, δ 1.87), and so is the imine proton signal (**1**, δ 6.10; **2**, δ 5.49), suggesting symmetric coordination of the R_2-dad ligands. The resonances of the imine protons are shifted to higher fields than those of free R_2-dad ligands in C_6D_6 (R = ^{i}Pr, δ 7.99; R = ^{t}Bu, δ 8.11), and their chemical shifts are consistent with an η^4-enediamido(2−) formulation.[5,6] The presence of diasterotopic $CHMe_2$ groups of **1** leads to two methyl doublets (δ 1.42 and 0.88) and one methine septet (δ 4.27). On the other hand, the *tert*-butyl groups of **2** give a singlet at δ 1.53. Irradiation of the Cp* methyl signal of **1** resulted in a significant nuclear Overhauser enhancement (NOE) (17.2%) of the methine signal. This observation indicates that the isopropyl groups of R_2-dad are in close proximity to the Cp* ligand by adopting a supine conformation, which is consistent with the X-ray-derived structure as will be shown later in this paper. For **2**, irradiation of the Cp* methyl signal did not cause a noticeable NOE enhancement, suggesting an alternative prone conformation. In the IR spectra of **1** and **2**, no appreciable N═C stretching band was observed.

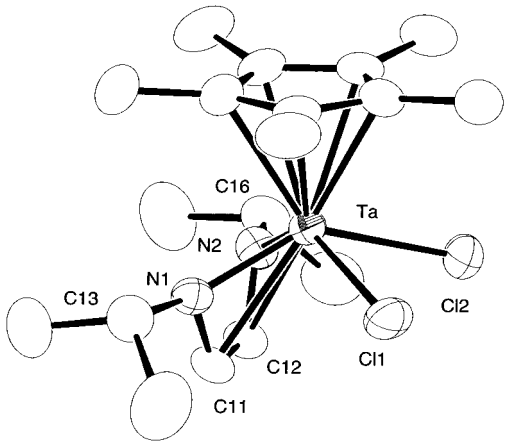

Figure 1. Molecular structure of Cp*Ta(^{i}Pr$_2$-dad)Cl_2 (**1**).

Table 1. Selected Bond Diastances (Å) and Angles (deg) of Cp*Ta(^{i}Pr$_2$-dad)Cl_2 (1), Cp*Ta(^{i}Pr$_2$-dad)(C≡CCMe$_3$)$_2$ (3), Cp*Ta(^{t}Bu$_2$-dad)(C≡C^{t}Bu)$_2$ (4) and Cp*Ta(^{i}Pr$_2$-dad)Me$_2$ (5)

	1	3	4	5
Ta−N1	2.000(4)	2.020(5)	2.046(3)	2.006(8)
Ta−N2	2.006(4)	2.040(5)	2.035(3)	2.025(8)
Ta−C11	2.430(5)	2.439(6)	2.463(3)	2.49(1)
Ta−C12	2.436(5)	2.441(6)	2.465(3)	2.494(9)
N1−C11	1.374(7)	1.362(8)	1.373(4)	1.37(1)
N2−C12	1.370(7)	1.354(8)	1.361(5)	1.36(1)
C11−C12	1.380(7)	1.381(9)	1.368(5)	1.37(1)
Ta−Cl1	2.490(2)			
Ta−Cl2	2.492(2)			
Ta−C(alkynyl, methyl)		2.200(7)	2.166(3)	2.23(1)
		2.198(7)	2.176(4)	2.22(1)
C≡C		1.187(9)	1.196(5)	
		1.201(9)	1.199(5)	
N1−Ta−N2	84.1(2)	82.6(2)	83.9(1)	83.9(3)
Cl1−Ta−Cl2	78.05(6)			
C−Ta−C(alkynyl, methyl)		76.6(2)	73.1(1)	74.9(4)
Ta−N1−C11	90.2(3)	90.1(4)	89.9(2)	93.2(5)
Ta−N2−C12	90.3(3)	89.7(4)	90.9(2)	92.8(6)
N1−C11−C12	118.3(5)	117.8(6)	119.9(3)	119.3(9)
N2−C12−C11	118.4(5)	119.3(6)	119.7(3)	118.8(8)
Ta−C≡C		172.7(5)	175.2(3)	
		176.7(5)	176.2(3)	

Crystal Structure of Cp*Ta(^{i}Pr$_2$-dad)Cl_2 (1). The molecular structure of **1** was determined by X-ray diffraction. Selected bond distances and angles are listed in Table 1. The molecular structure is shown in Figure 1. The ^{i}Pr$_2$-dad ligand of **1** is coordinated to the Ta atom in an η^4 fashion via two nitrogen and two inner carbon atoms, and the TaN_2C_2 five-membered ring is folded by 60.48° along the N−N vector. The complex **1** exhibits a supine conformation, where the ^{i}Pr substituents point toward the Cp* ligand. This coordination geometry is similar to those of (C_5H_5)Nb(^{t}Bu$_2$-dad)Cl_2 and (C_5H_5)Ta{$(C_6H_4-OCH_3\text{-p})_2$-dad}$Cl_2$.[7,9] In the case

(9) (a) Mashima, K.; Matsuo, Y.; Tani, K. *Chem. Lett.* **1997**, 767−768. (b) The synthesis of [η^5-$C_5H_3(SiMe_3)_2$]Ta[η^4-$C_6H_4(NSiMe_3)_2$-1,2]-Cl_2 was recently reported: Jiménez Pindado, G.; Thornton-Pett, M.; Bochmann, M. *J. Chem. Soc., Dalton Trans.* **1998**, 393−400.

(10) (a) tom Dieck, H.; Franz, K.-D. *Angew. Chem., Int. Ed. Engl.* **1975**, *14*, 249−250. (b) tom Dieck, H.; Zettlitzer, M. *Chem. Ber.* **1987**, *120*, 795−801.

of the $^tBu_2$-dad complex **2**, the NOE study is indicative of a prone conformation. This is not surprising considering the steric bulk of the *tert*-butyl group, which would collide with Cp* if the complex assumes a supine conformation. A similar steric argument was applied also to the conformational preference of substituted 1,3-diene ligands in Cp*Ti(diene)Cl.[11] However, electronic effects may not be ruled out for the geometrical choice.

The N1−C11 and N2−C12 distances of 1.374(7) and 1.370(7) Å are significantly longer than those of the R_2-dad ligands in Fe(CO)($^iPr_2$-dad)(2,3-$Me_2C_4H_4$) (1.311 Å), $PdCl_2$($^tBu_2$-dad)($C_6H_5CH{=}CH_2$) (1.28 Å), and free (cyclohexyl)$_2$-dad (1.258(5) Å).[12] On the other hand, the C11−C12 distance of 1.380(8) Å is short compared with the relevant structures: Fe(CO)($^iPr_2$-dad)(2,3-$Me_2C_4H_4$) (1.405(3) Å); $PdCl_2$($^tBu_2$-dad)($C_6H_5CH{=}CH_2$) (1.51(5) Å); free (cyclohexyl)$_2$-dad (1.457(2) Å).[13] The long N−C distances and concomitant short C−C distances provide evidence for the enediamido character of the $^iPr_2$-dad ligand in **2**. The Ta−N distances of 2.000(4) and 2.006(4) Å observed for **1** corroborate the above argument, which are close to the known Ta(V)−amido bonds and are definitely shorter than Ta−amine bonds.[14]

Reactions of Cp*Ta(R_2-dad)Cl_2 with LiC≡C^{t}Bu and MeMgI. The successful isolation of **1** and **2** prompted us to examine substitution reactions of the chloride ligands. We have found that addition of 2 equiv of LiC≡C^{t}Bu to the dichlorido complexes in THF followed by standard workup afforded Cp*Ta(R_2-dad)(C≡C^{t}Bu)$_2$ (R = ^{i}Pr (**3**), 45%; ^{t}Bu (**4**), 66%) as yellow crystals. While the analogous reactions of **1** and **2** with methyllithium did not give isolable products, we were able to isolate the methyl derivatives Cp*Ta(R_2-dad)Me_2 (R = ^{i}Pr (**5**), 40%; ^{t}Bu (**6**), 28%) from the reactions with 2 equiv of MeMgI in THF. In contrast to **1** and **2**, **3**−**6** are very soluble in hexane and toluene. These carbyl derivatives are air- and moisture-sensitive, but are thermally stable. They do not show any signs of decomposition in C_6D_6 at 80 °C for 2 days in the absence of air, according to their ^{1}H NMR spectra. It was reported that the related hafnium complex Cp*Hf($^iPr_2$-dad)Me reacted with propyne, CO, and H_2 to afford propynyl, acyl, and hydride derivatives, respectively.[6,15] However, the ^{1}H NMR experiments in C_6D_6 showed that **4** and **5** were inert toward 1 atm H_2, CO, and CO_2 at 30−80 °C and did not react with ^{t}BuNC and ^{t}BuC≡CH, too.

The carbyl complexes, **3**−**6**, were characterized by IR, ^{1}H, and ^{13}C{^{1}H} NMR spectra and combustion analyses. The IR spectra of the alkynyl complexes **3** and **4** show the C≡C stretching bands at 2090 and 2100 cm^{-1}, respectively. Both the ^{1}H and ^{13}C{^{1}H} NMR spectra show single resonances for the NCH and Cp* groups, and the chemical shifts of their dad resonances are

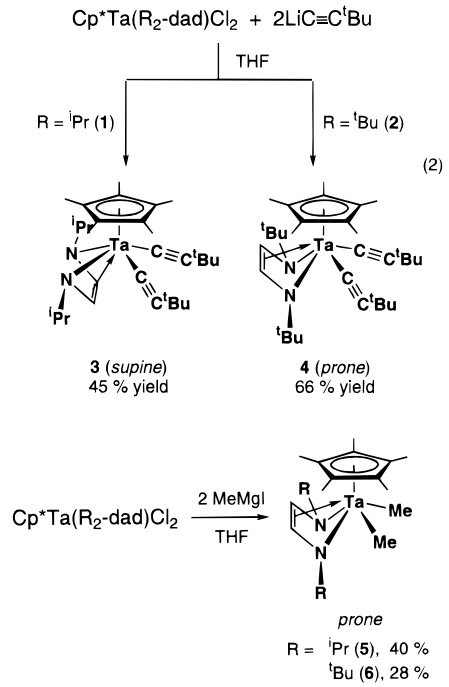

similar to those of **1** and **2**, indicating an η^4-coordination mode of the dad ligands in **3** and **4**. The Ta−CH_3 resonances in **5** (δ 0.43) and **6** (δ 0.62) are shifted to lower fields compared with Cp*Ta(η^4-1,3-diene)Me_2 (δ −0.69 and −0.43).[16] The NOE experiments by irradiation of the Cp* signal allowed us to predict the conformation of the R_2-dad ligands. For **3**, 12.0% NOE enhancement was observed for the methine protons of the isopropyl groups, which indicates a supine conformation. On the other hand, a prone conformation of **4**, **5**, and **6** was suggested by 12.1, 7.4, and 10.1% NOE enhancement of the imine protons. Thus, during the alkynylation and methylation reactions leading to **3**, **4**, and **6**, the orientation of $^tBu_2$-dad or $^iPr_2$-dad is retained. In contrast, on going from **1** to **5**, the flipping of the $^iPr_2$-dad coordination mode from the supine to the prone conformation takes place.

Crystal Structures of Cp*Ta($^iPr_2$-dad)(C≡C^{t}Bu)$_2$ (3), Cp*Ta($^tBu_2$-dad)(C≡C^{t}Bu)$_2$ (4), and Cp*Ta($^iPr_2$-dad)Me_2 (5). The molecular structures of **3**, **4**, and **5** were determined by X-ray diffraction, which are shown in Figures 2−4. The selected bond distances and angles are summarized in Table 1. In one ^{t}BuC≡C ligand of **3**, three methyl carbons of the *tert*-butyl group are disordered, with an occupancy factor of 50/50. In Figure 2, only one set of the disordered carbons is shown.

The five-membered chelate rings of the dad ligands in **3**−**5** are folded along the N−N vector by 61.6° (**3**), 58.8° (**4**), and 54.6° (**5**). It is confirmed that **3** adopts a supine geometry and **4** and **5** opt for an alternative prone geometry, as was suggested by the NOE experiments. The geometrical choice seems to be the consequence of a delicate balance of steric interactions between Cp*, carbyl groups, and the substituents of dad. The N−C and C−C distances of the dad ligand in **3**, **4**, and **5** resemble those of **1**, suggesting its enediamido character. The average Ta−N distances in **3** (2.030 Å), **4** (2.041 Å), and **5** (2.016 Å) are slightly longer than that

(11) Yamamoto, H.; Yasuda, H.; Tatsumi, K.; Lee, K.; Nakamura, A.; Chen, J.; Kai, Y.; Kasai, N. *Organometallics* **1989**, *8*, 105−119.
(12) (a) Frühauf, H. W.; Wolnershäusen, G. *Chem. Ber.* **1982**, *115*, 1070−1082. (b) van der Poel, H.; van Koten, G.; Vrieze, K.; Kokkes, M.; Stam, C. H. *J. Organomet. Chem.* **1979**, *175*, C21−C24.
(13) Keijsper, J.; van der Poel, H.; Polm, L. H.; van Koten, G.; Vrieze, K. *Polyhedron* **1983**, *2*, 1111−1116.
(14) Chisholm, M. H.; Huffman, J. C.; Tan, J.-S. *Inorg. Chem.* **1981**, *20*, 1859−1866.
(15) The reaction of Cp*Hf($^iPr_2$-dad)Cl with ^{t}BuNC was also reported to give Cp*Hf[^{i}PrNCH=CHNC(Me)=CHC(^{t}Bu)=NH]Cl: Bol, J. E.; Hessen, B.; Teuben, J. H.; Smeets, W. J. J.; Speck, A. L. *Organometallics* **1992**, *11*, 1981−1983.
(16) Mashima, K.; Fujikawa, S.; Nakamura, A. *J. Am. Chem. Soc.* **1993**, *115*, 10990−10991.

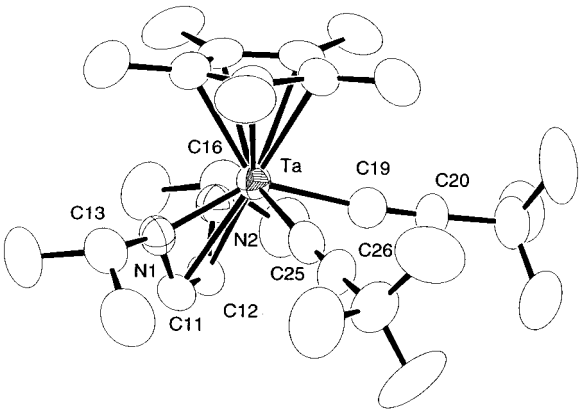

Figure 2. Molecular structure of Cp*Ta(^{i}Pr$_2$-dad)(C≡C^{t}Bu)$_2$ (**3**). One set of the disordered carbons of a ^{t}BuC≡C ligand is shown.

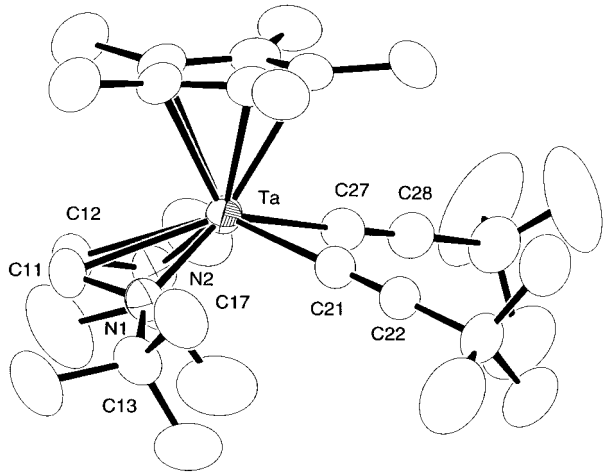

Figure 3. Molecular structure of Cp*Ta(^{t}Bu$_2$-dad)(C≡C^{t}Bu)$_2$ (**4**).

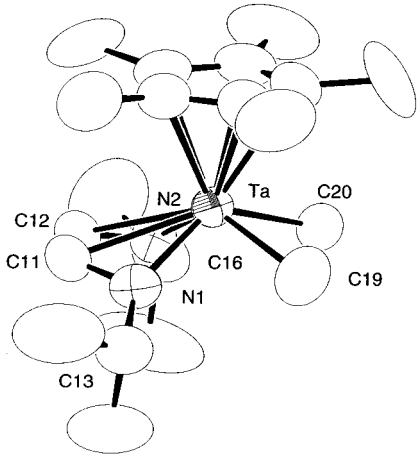

Figure 4. Molecular structure of Cp*Ta(^{i}Pr$_2$-dad)Me$_2$ (**5**).

of **1** (2.003 Å). A small but notable geometrical difference between the prone and supine dad ligands may be seen at the nitrogen atoms. The N-coordination of prone-dad in **4** and **5** occurs with a planar nitrogen geometry, where the sums of the angles about the N atoms are N1 = 359.4° and N2 = 359.5° for **4**, and N1 = 359.8° and N2 = 359.5° for **5**. On the other hand, the nitrogen atoms of supine-dad in **1** and **3** are slightly pyramidalized, with the corresponding angles being N1 = 353.0° and N2 = 352.8° for **1**, and N1 = 352.0° and N2 = 353.3° for **3**. The nonplanarity of the nitrogen atoms of supine-dad then may be a consequence of steric repulsion between the isopropyl substituents and the Cp* ligand.

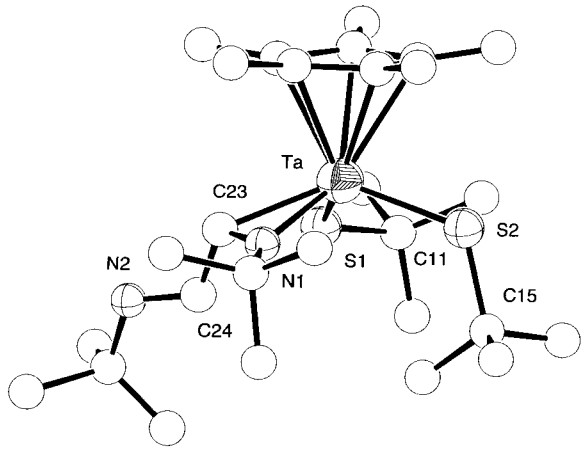

Figure 5. Molecular structure of Cp*Ta(^{t}Bu$_2$-dad)(S^{t}Bu)$_2$ (**7**).

The Ta−CH$_3$ distances of 2.23(1) and 2.22(1) Å in **5** are comparable to the known Ta−CH$_3$ distances (2.16−2.25 Å)[17] and are longer than the average of the Ta−C(alkynyl) distances of 2.199 Å in **3** and 2.171 Å in **4**. The C≡C distances of **3** and **4** fall in the normal range of triple bonds (1.18−1.25 Å),[18] and the Ta−C≡C spines are nearly linear.

Reaction of Cp*Ta(^{t}Bu$_2$-dad)Cl$_2$ (2) with LiS^{t}Bu. We then examined the reaction of the ^{t}Bu$_2$-dad complex **2** with LiS^{t}Bu, anticipating that the bulky thiolate ligand might affect the coordination mode of R$_2$-dad. While the reaction of **2** with 2 equiv of LiS^{t}Bu in THF gave no isolable products, Cp*Ta(^{t}Bu$_2$-dad)(S^{t}Bu)$_2$ (**7**) was obtained as orange crystals in 58% yield when the amount of LiS^{t}Bu was increased to 4 equiv. Complex **7** is air- and moisture-sensitive, is very soluble in common organic solvents, and is crystallized from pentane.

The formulation of **7** was inferred from the spectroscopic data and combustion analysis, and the preliminary structure data were obtained by X-ray analysis. Although poor quality of the crystal prevents us from discussing its metric parameters in detail, the refinement clearly showed the molecular structure of **7**, which is presented in Figure 5.[19] The molecule consists of a

(17) (a) Guggenberger, J. L.; Schrock, R. R. *J. Am. Chem. Soc.* **1975**, *97*, 6578−6579. (b) McLain, S. J.; Schrock, R. R.; Sharp, P. R.; Churchill, M. R.; Youngs, W. J. *J. Am. Chem. Soc.* **1979**, *101*, 263−265. (c) Churchill, M. R.; Youngs, W. *Inorg. Chem.* **1979**, *18*, 1697−1702. (d) Freundlich, J. S.; Schrock, R. R.; Cummins, C. C.; Davis, W. M. *J. Am. Chem. Soc.* **1994**, *116*, 6476−6477. (e) Gómez, M.; Jimenez, G.; Royo, P.; Pelinghelli, M. A.; Tiripicchio, A. *J. Organomet. Chem.* **1992**, *439*, 309−318. (f) Mashima, K.; Fujikawa, S.; Tanaka, Y.; Urata, H.; Oshiki, T.; Tanaka, E.; Nakamura, A. *Organometallics* **1995**, *14*, 2633−2640. (g) Mashima, K.; Tanaka, Y.; Nakamura, A. *Organometallic* **1995**, *14*, 5642−5651.

(18) (a) Akita, M.; Terada, M.; Oyama, S.; Moro-oka, Y. *Organometallics* **1990**, *9*, 816−825. (b) Erker, G.; Frömberg, W.; Benn, R.; Mynott, R.; Angermund, K.; Krüger, C. *Organometallics* **1989**, *8*, 911−920. (c) Kawaguchi, H.; Tatsumi, K. *Organometallics* **1995**, *14*, 4294−4299. (d) Nast, R. *Coord. Chem. Rev.* **1982**, *47*, 89−124. (e) *Advanced Organic Chemistry*; March, J. W., Ed.; Wiley: New York, 1985.

(19) Crystals of Cp*Ta(^{t}Bu$_2$-dad)(S^{t}Bu)$_2$ (**7**) are triclinic, $P\bar{1}$ (No. 2), with a = 12.769(9) Å, b = 16.87(1) Å, c = 9.52(1) Å, α = 104.33(8)°, β = 105.00(6)°, γ = 96.99(7) Å, V = 1881(3) Å^3, and Z = 2; 148 parameters were refined on 5824 reflections having $I > 3\sigma(I)$; R (R_w) = 0.128 (0.186), GOF = 7.95.

Table 2. Crystallographic Data for Cp*Ta(^{i}Pr$_2$-dad)Cl$_2$ (1), Cp*Ta(^{i}Pr$_2$-dad) (C≡C^{t}Bu)$_2$ (3), Cp*Ta(^{t}Bu$_2$-dad)(C≡C^{t}Bu)$_2$ (4), and Cp*Ta(^{i}Pr$_2$-dad)Me$_2$ (5)

	1	3	4	5
formula	$C_{18}H_{31}N_2TaCl_2$	$C_{30}H_{49}N_2Ta$	$C_{32}H_{53}N_2Ta$	$C_{20}H_{37}N_2Ta$
mol wt (g mol^{-1})	527.31	618.68	646.73	468.48
cryst syst	monoclinic	monoclinic	triclinic	monoclinic
space group	$P2_1/n$(No. 14)	$P2_1/n$(No. 14)	$P\bar{1}$ (No. 2)	$P2_1/c$(No. 14)
color of cryst	yellow	yellow	yellow	yellow
cryst size (mm)	0.20 × 0.25 × 0.20	0.35 × 0.20 × 0.70	0.25 × 0.33 × 0.50	0.70 × 0.50 × 0.10
a (Å)	9.931(3)	11.286(6)	9.579(1)	9.180(1)
b (Å)	14.512(3)	20.09(1)	19.831(3)	13.449(3)
c (Å)	14.447(2)	14.790(9)	9.324(2)	18.403(4)
α (deg)			90.72(1)	
β (deg)	100.34(2)	112.06(3)	109.86(1)	75.26(1)
γ (deg)			102.63(1)	
V (Å^3)	2048.3(9)	3108(2)	1618.2(5)	2197.3(8)
Z	4	4	2	4
ρ_{calc} (g cm^{-3})	1.710	1.322	1.327	1.470
μ (Mo Kα) (cm^{-1})	56.20	35.48	34.11	49.98
$2\theta_{max}$ (deg)	55	50	55	55
abs range	0.75−1.000	0.57−1.00	0.91−1.00	0.30−1.00
no. of unique rflns	4885	5662	7890	5260
no. of obs data[a,b]	3735	3701	6557	3109
no. of params	209	326	317	209
residuals (R/R_w)[c]	0.029/0.036	0.035/0.039	0.024/0.029	0.046/0.061
GOF[d]	1.53	1.71	1.60	1.97

[a] At room temperature. [b] Observation criterion $I > 3\sigma(I)$. [c] $R = \sum||F_o| - |F_c||/\sum|F_o|$. $R_w = [\{\sum w(|F_o| - |F_c|)^2\}/\sum wF_o^2]^{1/2}$. [d] GOF = $[\{\sum w(|F_o| - |F_c|)^2\}/(N_o - N_p)]^{1/2}$, where N_o and N_p denote the numbers of data and parameters.

Ta atom surrounded by Cp*, dad, and two thiolato ligands. The most remarkable feature of **7** is that the ^{t}Bu$_2$-dad ligand is bound to the Ta atom in an η^2 mode at one imine N═C site. Complex **7** provides a rare example of the η^2-*N*,*C*-coordinated early transition metal complex of dad. This unusual coordination mode was previously found in the structure of Nb$_2$(^{t}Bu$_2$-dad)$_5$.[8] The slide of ^{t}Bu$_2$-dad from the symmetric η^4-σ^2,π-coordination geometry to the unsymmetric η^2-*N*,*C* geometry is probably a consequence of the steric congestion induced by the bulky ^{t}BuS groups. The solid-state structure of **7** is retained in solution, according to its ^{1}H NMR spectrum. Four different *tert*-butyl signals of equal intensity appeared, and the imine protons were observed as two doublets. The doublet of the uncoordinated imine proton appears at δ 7.99, which is similar to that of free ^{t}Bu$_2$-dad. On the other hand, the doublet of the η^2 coordinated imine proton is largely shifted to higher field and appears at δ 3.62. The IR spectrum also indicates the presence of an uncoordinated imine group, showing a strong band at 1620 cm^{-1} assignable to the N═CH vibrational mode. Free ^{t}Bu$_2$-dad exhibits the corresponding IR band at 1630 cm^{-1}.

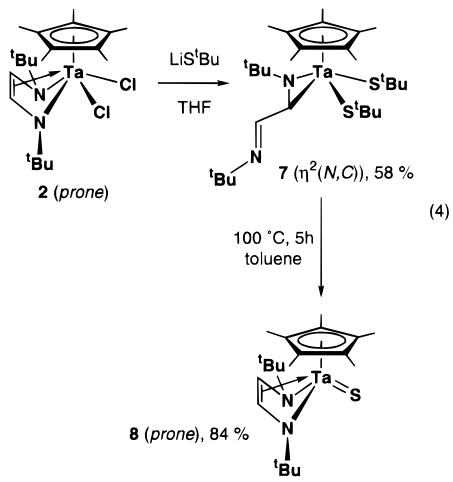

(4)

The thiolato complex **7** is not thermally stable in solution. Upon heating a benzene-d_6 solution of **7** at 80 °C in a sealed tube, we noticed the formation of a new complex according to the ^{1}H NMR spectra, which also indicated the presence of the same amounts of HS^t-Bu and isobutene. This complex turned out to be Cp*Ta(^{t}Bu$_2$-dad)(S) (**8**) as described below. On a preparative scale, complex **8** was obtained in 84% yield from a toluene solution of **7** by stirring it at 100 °C for 4 h. This thermal reaction caused a color change from orange to yellow, and yellow needles of **8** were readily isolated. Spectra data and combustion analysis were consistent with the formulation of Cp*Ta(^{t}Bu$_2$-dad)(S). In the IR spectrum, the characteristic Ta═S stretching band was observed at 460 cm^{-1}, being comparable to those of the known tantalum sulfido complexes.[20] The EI mass spectrum consists of the parent molecular ion and fragment cations arising from loss of the *tert*-butyl group and the ^{t}Bu$_2$-dad ligand of **8**. The ^{1}H NMR spectrum suggests a symmetric nature of the ^{t}Bu$_2$-dad coordination, and irradiation of the Cp* methyl signal gives 5.6% NOE enhancement for the imine protons. Thus the σ^2,π-coordination mode of the ^{t}Bu$_2$-dad with a prone conformation is resumed during the reaction from **7** to **8**.

tert-Butylthiolate is known to undergo C−S bond cleavage occasionally at transition metal centers.[21] In the case of the thermal reaction of **7**, the C−S bond activation seems to be driven by the favorable change in coordination mode of ^{t}Bu$_2$-dad from η^2-*N*,*C* to η^4-σ^2,π. By the same reason, dinucleation and cluster formation of the resulting sulfide complex **8** are prevented. The

(20) (a) Sola, J.; Do, Y.; Berg, J. M.; Holm, R. H. *Inorg. Chem.* **1985**, *24*, 1706−1713. Lee, S. C.; Li, J.; Mitchell, J. C.; Holm, R. H. *Inorg. Chem.* **1992**, *31*, 4333−4338. (b) Schreiner, S.; Aleandri, L. E.; Kang, D.; Ibers, J. A. *Inorg. Chem.* **1989**, *28*, 393−395. (c) Drew, M. G. B.; Rice, D. A.; Williams, D. M. *J. Chem. Soc., Dalton Trans.* **1984**, 845−848. (d) Kawaguchi, H.; Tatsumi, K. *Organometallics* **1997**, *16*, 307−309. (e) Tatsumi, K.; Inoue, Y.; Kawaguchi, H.; Kohsaka, M.; Nakamura, A.; Cramer, R. E.; VanDoorne, W.; Taogoshi, G. J.; Richmann, P. N. *Organometallics* **1993**, *12*, 352−364. (f) Bach, H.-J.; Brunner, H.; Wachter, J.; Nuber, B.; Ziegler, M. L. *Organometallics* **1992**, *11*, 1403−1407.

geometrical flexibility of R_2-dad would provide a new aspect of the role of ancillary ligands in transition-metal-assisted stoichiometric and catalytic reactions.

Experimental Section

General Comments. All reactions were performed under an argon atmosphere, using a standard Schlenk technique. THF, hexane, and toluene were distilled form Na/benzophenone. Cp*$TaCl_4$, R_2-dad (R = ^{t}Bu, ^{i}Pr), and LiC≡C^{t}Bu were synthesized according to the literature procedures.[22−24] MeMgI was prepared from methyl iodide and magnesium in diethyl ether. LiS^{t}Bu was obtained by the reaction of HS^{t}Bu with ^{n}BuLi in THF at 0 °C. NMR spectra were recorded on a Varian UNITYplus-500 spectrometer, and chemical shifts were reported in ppm by reference to deuterated solvents.

Preparation of Li_2(R_2-dad). In a typical reaction, a THF (10 mL) solution of ^{t}Bu_2-dad (0.49 g, 2.90 mmol) was treated with an excess of rodlike lithium metal (60 mg, 8.70 mmol). The solution was stirred at room temperature for 17 h, during which time the color of the solution gradually became dark red. The resulting dark red solution of Li_2(^{t}Bu_2-dad) and analogously prepared Li_2(^{i}Pr_2-dad) were used in the synthesis of **1** and **2**.

Preparation of Cp*Ta(^{i}Pr_2-dad)Cl_2 (1). A THF (10 mL) solution of Li_2(^{i}Pr_2-dad) (2.67 mmol) was added dropwise to Cp*$TaCl_4$ (1.22 g, 2.66 mmol) in THF (20 mL) at 0 °C. The reaction mixture was stirred at room temperature for 24 h, during which time yellow microcrystals of **1** precipitated. The solvent was then reduced in volume to ca. 15 mL, which was stored in a refrigerator at −20 °C. The product **1** was isolated as yellow crystals (1.06 g, 76%). ^{1}H NMR (C_6D_6): δ 6.10 (s, 2H, NC*H*), 4.27 (septet, 2H, C*H*Me_2), 2.07 (s, 15H, C_5*Me*$_5$), 1.42 (d, 3H, CH*Me*Me), 0.88 (d, 3H, CHMe*Me*). Anal. Calcd for $C_{18}H_{31}N_2Cl_2Ta$: C, 41.00; H, 5.93; N, 5.31. Found: C, 40.67; H, 5.83; N, 5.18.

Preparation of Cp*Ta(^{t}Bu_2-dad)Cl_2 (2). A THF (10 mL) solution of Li_2(^{t}Bu_2-dad) (2.49 mmol) was added dropwise to Cp*$TaCl_4$ (1.14 g, 2.49 mmol) in THF (20 mL) at 0 °C. The dark red solution was stirred at room temperature for 2 h. After removal of solvent in vacuo, the dark red residue was treated with toluene (40 mL). The toluene solution was centrifuged to remove LiCl and was evaporated to dryness. The resulting dark red solid was recrystallized from DME (40 mL) to yield orange needles of **2** (1.51 g, 54%). ^{1}H NMR (C_6D_6): δ 5.49 (s, 2H, NC*H*), 1.87 (s, 15H, C_5*Me*$_5$), 1.53 (s, C*Me*$_3$). MS (EI, *m*/*z*): 555 (M^+), 497 (M^+ − CMe_3), 441 (M^+ − 2CMe_3), 387 (M^+ − ^{t}Bu-dad). Anal. Calcd for $C_{20}H_{35}N_2Cl_2Ta$: C, 43.25; H, 6.35; N, 5.04. Found: C, 43.53; H, 6.58; N, 5.04.

Preparation of Cp*Ta(^{i}Pr_2-dad)(C≡C^t$Bu)_2$ (3). A THF (10 mL) solution of LiC≡C^{t}Bu (1.98 mmol) was added to a yellow slurry of **1** (0.52 g, 0.99 mmol) in THF (50 mL) at −78 °C. Upon warming to room temperature, the reaction mixture became a homogeneous dark red solution. This solution was stirred for 13 h, and the solvent was removed in vacuo. The residue was treated with hexane (25 mL). After LiCl was removed by centrifugation, the hexane solution was concentrated to ca. 5 mL. From this concentrated solution, yellow **3** crystallized at −20 °C (0.28 g, 45%). ^{1}H NMR (C_6D_6): δ 5.75 (s, 2H, NC*H*), 4.86 (septet, 2H, C*H*Me_2), 2.09 (s, 15H, C_5*Me*$_5$), 1.46 (s, 18H, C*Me*$_3$), 1.30 (d, 3H, CH*Me*Me), 1.17 (d, 3H, CHMe*Me*). ^{13}C{^{1}H} NMR (C_6D_6): δ 138.3 (*C*≡CCMe$_3$), 123.2 (C≡*C*CMe$_3$), 116.1 (C_5Me$_5$), 101.4 (N*C*H), 54.3 (*C*HMe_2), 32.7 (C*Me*$_3$), 29.4 (*C*Me$_3$), 24.8 (CH*Me*Me), 24.16 (CHMe*Me*), 12.6 (C_5*Me*$_5$). IR (Nujol): 2090 (s, C≡C) cm^{-1}. MS (EI, *m*/*z*): 618 (M^+), 561 (M^+ − ^{t}Bu), 456 (M^+ − 2 CC^{t}Bu). Anal. Calcd for $C_{30}H_{49}N_2Ta$: C, 58.24; H, 7.98; N, 4.53. Found: C, 57.83; H, 8.23; N, 4.50.

Preparation of Cp*Ta(^{t}Bu_2-dad)(C≡C^t$Bu)_2$ (4). LiC≡C^{t}Bu (0.78 mmol) in THF (5 mL) was added to a THF (30 mL) solution of **2** (0.22 g, 0.40 mmol) at 0 °C. After stirring at room temperature for 13 h, the resulting orange solution was evaporated to dryness. The orange residue was extracted with toluene (10 mL). The toluene solution was centrifuged to remove insoluble LiCl. Removal of the solvent in vacuo left an orange solid, which was recrystallized from DME to afford **4** as yellow crystals (0.17 g, 66%). ^{1}H NMR (C_6D_6): δ 5.55 (s, 2H, NC*H*), 1.99 (s, 15H, C_5*Me*$_5$), 1.60 (s, 18H, C*Me*$_3$), 1.52 (s, 18H, C*Me*$_3$). ^{13}C{^{1}H} NMR (C_6D_6): δ 139.1 (*C*≡CCMe$_3$), 126.5 (C≡*C*CMe$_3$), 115.1 (C_5Me$_5$), 100.3 (N*C*H), 60.7 (N*C*Me$_3$), 33.3 (C*Me*$_3$), 32.3 (C*Me*$_3$), 29.7 (C≡C*C*Me$_3$), 12.8 (C_5*Me*$_5$). IR (Nujol): 2100 (s, C≡C) cm^{-1}. MS (EI, *m*/*z*): 646 (M^+), 589 (M^+ − ^{t}Bu), 484 (M^+ − 2 CC^{t}Bu). Anal. Calcd for $C_{32}H_{53}N_2Ta$: C, 59.43; H, 8.26; N, 4.33. Found: C, 59.17; H, 8.70; N, 4.34.

Preparation of Cp*Ta(^{t}Pr_2-dad)Me_2 (5). To a yellow slurry of **1** (1.12 g, 2.11 mmol) in THF (60 mL) was added an Et_2O (6.8 mL) solution of MeMgI (4.22 mmol) at −78 °C. The yellow slurry was allowed to warm to room temperature and was stirred for 13 h. After the solution was centrifuged to remove magnesium salts, the volatiles were removed in vacuo. The residue was recrystallized from HMDSO to yield **5** as orange crystals (0.41 g, 40%). ^{1}H NMR (C_6D_6): δ 5.58 (s, 2H, NC*H*), 4.30 (septet, 2H, C*H*Me_2), 1.72 (s, 15H, C_5*Me*$_5$), 1.12 (d, 3H, CH*Me*Me), 1.03 (d, 3H, CHMe*Me*), 0.43 (s, 6H, Ta*Me*). ^{13}C{^{1}H} NMR (C_6D_6): δ 112.5 (C_5Me$_5$), 99.0 (N*C*H), 50.2 (*C*HMe_2), 44.0 (Ta−*Me*), 26.6 (CH*Me*Me), 22.4 (CHMe*Me*), 12.8 (C_5*Me*$_5$). MS (EI, *m*/*z*): 471 (M^+ − Me). Anal. Calcd for $C_{20}H_{37}N_2Ta$: C, 49.38; H, 7.67; N, 5.76. Found: C, 49.02; H, 7.91; N, 5.69.

Preparation of Cp*Ta(^{t}Bu_2-dad)Me_2 (6). A yellow homogeneous solution of **2** (0.26 g, 0.48 mmol) in THF (20 mL) was treated with MeMgI (0.96 mmol) in Et_2O (0.68 mL) as described for the synthesis of **5**. The product **6** was isolated as yellow crystals (68 mg, 28%). ^{1}H NMR (C_6D_6): δ 5.47 (s, 2H, NC*H*), 1.69 (s, 15H, C_5*Me*$_5$), 1.40 (s, 18H, C*Me*$_3$), 0.62 (s, 6H, Ta*Me*). ^{13}C{^{1}H} NMR (C_6D_6): δ 112.3 (C_5Me$_5$), 101.0 (N*C*H), 60.7 (N*C*Me$_3$), 42.7 (Ta−*Me*), 33.4 (C*Me*$_3$), 11.7 (C_5*Me*$_5$). MS (EI, *m*/*z*): 499 (M^+ − Me). Anal. Calcd for $C_{18}H_{32}N_2Ta$: C, 51.36; H, 8.03; N, 5.44. Found: C, 50.19; H, 7.78; N, 5.14.

Preparation of Cp*Ta(^{t}Bu_2-dad)(S^t$Bu)_2$ (7). A THF (10 mL) solution of LiS^{t}Bu (1.02 mmol) was added to an orange solution of **2** (0.14 g, 0.25 mmol) in THF (20 mL) at 0 °C. The solution gradually turned deep in color, and it was warmed to room temperature. After the mixture was stirred for 1 h, the solution was evaporated to dryness. The resulting residue was extracted with hexane (5 mL), and LiCl was removed by centrifugation. The hexane solution was removed in vacuo, leaving an orange solid. This solid was crystallized from pentane to give **7** as orange crystals (97 mg, 58%). ^{1}H NMR (C_6D_6): δ 7.99 (d, 1H, NC*H*), 3.62 (d, br, 1H, NC*H*), 2.01 (s, 15H, C_5*Me*$_5$), 1.71 (s, 9H, C*Me*$_3$), 1.60 (s, 9H, C*Me*$_3$), 1.57 (s, 9H, C*Me*$_3$), 1.41 (s, 9H, C*Me*$_3$). IR (Nujol): 1620 (s, C=N) cm^{-1}. Anal. Calcd for $C_{28}H_{53}N_2S_2Ta$: C, 50.74; H, 8.06; N, 4.23; S, 9.68. Found: C, 50.31; H, 8.53; N, 3.61; S, 10.33. Due to thermal instability of **7**, repeated recrystallization caused partial decomposition of **7** into **8**.

(21) (a) Kawaguchi, H.; Yamada, K.; Lang, J.-P.; Tatsumi, K. *J. Am. Chem. Soc.* **1997**, *119*, 10346−10358. (b) Kawaguchi, H.; Yamada, K.; Ohnishi, S.; Tatsumi, K. *J. Am. Chem. Soc.* **1997**, *119*, 10871−10872. (c) Coucouvanis, D.; Hadjikyriacou, A. Lester, R.; Kanatzidis, M. G. *Inorg. Chem.* **1994**, *33*, 3645−3655. (d) Coucouvanis, D.; Chen, S.-J.; Mandimutsira, B. S.; Kim, C. G. *Inorg. Chem.* **1994**, *33*, 4429−4430. (e) Mandimutsira, B. S.; Chen, S.-J.; Demadis, K. D.; Coucouvanis, D. *Inorg. Chem.* **1995**, *34*, 2267−2268. (f) Kamata, M.; Yoshida, T.; Ohtsuka, S.; Hirotsu, K.; Higuchi, T. *J. Am. Chem. Soc.* **1981**, *103*, 3572−3574. (g) Piers, W. E.; Koch, L.; Ridge, D. S.; MacGillivray, L. R.; Zaworotko, M. *Organometallics* **1992**, *11*, 3148−3152.

(22) Okamoto, T.; Yasuda, H.; Nakamura, A.; Kai, Y.; Kanehisa, N.; Kasai, N. *J. Am. Chem. Soc.* **1988**, *110*, 5008−5017.

(23) *Preparative Acetylenic Chemistry*; Brandsma, L., Ed.; Elsevier: Amsterdam, 1971.

(24) Kliegman, J. M.; Barnes, R. K. *Tetrahedron* **1970**, *26*, 2555−2560.

Thermolysis of Cp*Ta(^{t}Bu$_2$-dad)(S^{t}Bu)$_2$ (7). A toluene (1 mL) solution of **7** (55 mg, 0.083 mmol) was stirred for 5 h at 100 °C. The color of the solution changed from orange to yellow. After removal of volatiles in vacuo, the residue was extracted into hexane (1 mL). Concentration and cooling of the hexane solution to −20 °C afforded Cp*Ta(^{t}Bu$_2$-dad)(S) (**8**) as yellow needles (36 mg, 84%). ^{1}H NMR (C_6D_6): δ 5.54 (s, 2H, NC*H*), 1.86 (s, 15H, C_5Me_5), 1.32 (s, 18H, CMe_3). ^{13}C{^{1}H} NMR (C_6D_6): δ 116.1 (C_5Me_5), 104.9 (N*C*H), 57.0 (N*C*Me$_3$), 32.1 (CMe_3), 12.8 (C_5Me_5). IR (Nujol): 460 (s, Ta═S) cm^{-1}. MS (EI, *m*/*z*): 516 (M$^+$), 404 (M$^+$ − 2^{t}Bu), 347 (M$^+$ − ^{t}Bu-dad). Anal. Calcd for $C_{20}H_{35}N_2STa$: C, 46.51; H, 6.83; N, 5.42; S, 6.21. Found: C, 46.57; H, 7.11; N, 5.22; S, 5.97.

Crystal Structure Determination of 1, 3, 4, 5, and 7. Crystals of **1**, **3**, **4**, **5**, and **7** suitable for X-ray analysis were mounted in glass capillaries and sealed under argon. Diffraction data were collected at room temperature on a Rigaku AFC7R diffractometer employing graphite-monochromated Mo Kα radiation (λ = 0.710690 Å) and using the ω−2θ scan technique. Refined cell dimensions and their standard deviations were obtained from least-squares refinements of 25 randomly selected centered reflections. Three standard reflections, monitored periodically for crystal decomposition or movement, showed only slight decline during the data collections for **1**, **3**, **4**, and **5**. In the case of **7**, 12% decay of standard reflections was observed over the 32.9 h period of data collection. The raw intensity data were corrected for Lorentz and polarization effects, and empirical absorption corrections based on ψ scans were applied.

All calculations were performed with the TEXSAN program package. The structures of **1**, **3**, **4**, **5**, and **7** were solved by direct methods, and the tantalum position was unequivocally located. Except for **7**, the remaining atoms were found in subsequent Fourier maps, and the structures were refined by full-matrix least squares. Anisotropic refinements were applied to all non-hydrogen atoms. The hydrogen atoms on the two imine groups were found in the Fourier maps, while the other hydrogens were put at calculated positions (C−H, 0.97 Å). For **3**, three carbons of a *tert*-butyl group of one alkynyl ligand are disordered, with occupancy factors of 50:50, and no hydrogen atom of its *tert*-butyl group was included. In the case of **7**, the Ta and S atoms were refined anisotropically, and all carbon atoms were refined isotropically. Crystals of **7** contain free ^{t}Bu$_2$-dad molecules, which could not be refined completely due to poor quality of the crystal. Additional information is available as Supporting Information.

Supporting Information Available: Tables for crystallographic data, positional parameters, bond distances and angles, and anisotropic thermal parameters for **1**, **3**, **4**, **5**, and **7** (34 pages). Ordering information is given on any current masthead page.

OM980319G